

Observations of Ductile Fracture Processes under Very Low Triaxiality in Quenched and Tempered VAR Steel and Preliminary Interpretation

Authors: Daniele Cannizzaro¹, Jacques H. Giovanola^{1,*},
Roberto Doglione², Andreas Rossoll³

1) Graduate student, respectively Professor, Laboratoire de Conception des Systèmes Mécaniques, Ecole Polytechnique Fédérale de Lausanne (Switzerland), 2) Professor, Politecnico di Torino (Italy), 3) Senior Scientist, Laboratoire de Métallurgie Mécanique, Ecole Polytechnique Fédérale de Lausanne (Switzerland). *) Corresponding author

ABSTRACT

This paper presents preliminary results of an investigation aimed at understanding and modeling ductile fracture of clean heat-treatable high strength steels, particularly under low triaxiality loading conditions. Results of torsion and tension/torsion experiments are presented and complemented by detailed fractographic observations. We find that ductile fracture under low (0 to 0.15) as well as higher triaxiality loading is controlled by void nucleation at tempering carbides. Once nucleated voids grow and coalesce without significant additional macroscopic deformation. We apply the dislocation model proposed by Kwon and Asaro to calculate the carbide-matrix interface stress as a function of plastic strain and mean stress. Using our experimental torsion and tension/torsion data, we obtain estimates of the critical nucleation stress ranging from 1880 to 2140 MPa for the range of triaxialities investigated. These values are consistent with values reported in the literature for other steels and their relatively narrow range suggests that the Kwon-Asaro model may be used to predict void nucleation at carbides for low as well as for high triaxialities.

1 INTRODUCTION

The motivation for the research presented in this paper is twofold. First, current engineering problems increasingly require the prediction of fracture conditions in uncracked metallic parts for loading conditions affording low or very low stress triaxiality. Unfortunately the ability of existing fracture mechanics methodologies and damage models to predict the onset of fracture under low triaxiality conditions is still limited; significant progress has been made in the modelling of void growth under those conditions, with some effort to provide a better characterization of void coalescence [1-4]. Second, the quality and cleanliness of metallic alloys improves continuously, particularly for heat-treatable high-strength steels where modern metallurgical practices such as vacuum-arc-remelting (VAR) drastically reduce the volume fraction of detrimental inclusions such as manganese sulfides or oxides. In these alloys, small particles, mainly carbides, play a more prominent role in controlling fracture processes. Because tempering carbides are usually densely spaced and tightly bonded to the matrix, void nucleation at carbides may influence the total fracture process much more strongly than for fracture in alloys where voids nucleate and grow at easily debonded or broken, and more widely spaced inclusions.

In light of these remarks, the specific research objectives underlying this paper are:

- 1) to characterize qualitatively and as quantitatively as feasible the ductile fracture processes in a VAR heat-treatable steel subjected to low triaxiality loading conditions and
- 2) to improve existing micromechanical damage models or develop suitable new ones to account for experimental observations and make reliable fracture predictions.

Broader, longer term objectives are to elucidate and model the influence of inclusion type (small hard tightly bonded, densely distributed or large soft or brittle more widely spaced), strength level and hardening rate on fracture under quite general geometric conditions (cracked, notched, or plain material) and loading conditions, with a view towards establishing fracture scaling rules for engineering applications (see discussion in Giovanola et al. [5,6]). This paper presents the current status of this investigation. The next section describes the selected approach. Section 3 presents fracture test data and metallographic and fractographic observations, whereas Section 4 discusses these results and provides a preliminary interpretation. Finally, Section 5 concludes with the significance of the results and an outline of future research.

2 RESEARCH APPROACH

To reach the two objectives specified above we are applying the following approach. We selected a hardenable VAR steel (Aubert-Duval NC40MW), and heat-treated it to obtain a dispersion of tempering carbides in a soft ferritic matrix (austenitized for 1 hrs at 860°C, quenched in oil and tempered in air for 1 hrs at 704°C). The chemical composition of the steel is given in Table 1, whereas Table 2 lists its mechanical properties, obtained in smooth round bar tensile tests.

Table 1: Chemical Composition of Investigated Steel

C	Si	Mn	S	P	Ni	Cr	Mo	Cu	Fe
0.399	0.28	0.72	<0.002	<0.005	1.79	0.84	0.23	0.03	Bal.

Table 2: Mechanical Properties of Investigated Steel*

Yield strength [MPa]	Tensile Strength [Mpa]	Elongation to fracture [%]	Reduction of Area [%]
700	800	20	37.5

*(specimen made from a round bars oriented along the extrusion direction L, diameter 4 mm, gauge length 24 mm)

We characterized the microstructure metallographically and in particular measured and calculated its carbide and MnS contents and distributions. We then designed and fabricated thin-walled cylindrical specimens suitable for pure torsion (T) and tension-torsion (TT) experiments. The design of the specimen was validated by performing a finite deformation, elasto-plastic finite elements simulation (up to 30% shear strain) that demonstrated uniformity of the stress and strain distributions along the axial direction of the specimen. To avoid stress concentrations, we polished the outside surface of the specimens. We performed T and TT tests with these specimens using a servo-hydraulic tension-torsion machine. During the experiments, we recorded the rotation and the axial displacement of the actuated ram as well as the axial load and torque applied to the specimen. We also took photographs of the deforming gage section on which axial fiduciary lines had been drawn with a pen before the test. The T experiments were performed under rotation control at a rotation rate of $1.4 \cdot 10^{-3}$ rad/s. For the TT experiments, we first applied a load of 34 kN (about 40% of the yield load for a triaxiality of around 0.15), which was held constant during the test, and then loaded the specimen in torsion with a rotation rate of $1.4 \cdot 10^{-3}$ or $7 \cdot 10^{-3}$ rad/s. For both types of experiments, we either loaded the specimens to unstable fracture, or interrupted the test just after the onset of significant softening. After the experiments, selected specimens were metallographically prepared for inspection by scanning electron microscopy in order to establish and, when feasible, quantify micro damage processes leading to fracture.

3 RESULTS

Microstructural Characterization

The quenching produces a lower bainite microstructure; subsequent tempering leads to a dispersion of carbides (mainly cementite) in a ferritic matrix. From the carbon content, we calculated a carbide volume fraction of 6.1%. 2D quantitative image analysis provided a mean carbide size on the order of 0.23 μm with some carbides as small as 0.1 μm and some as large as 1 μm , and a mean aspect ratio of 2.4. The alloy contains only few randomly distributed MnS inclusions (volume fraction f of about $5 \cdot 10^{-5}$ as estimated by Franklin's formula).

Loading curves for the T and TT Experiments

Figure 1 presents the applied torque versus rotation angle curves for the T and TT experiments, respectively. For the TT experiments, Fig 1b also shows the axial displacement versus rotation angle undergone by the specimens. The unloading around 40° in Fig 1a was mandated by the limited rotational range of the machine. In the specimens tested to unstable fracture, a through-wall crack propagated around part of the circumference (in a plane more or less perpendicular to the specimen axis) and arrested. For T experiments, there is considerable scatter in the maximum rotation angle (66° to 84° corresponding to an average engineering shear strain of $\gamma = 1.90 - 2.43$), whereas for TT experiments, we observe much less scatter in the final deformation data (rotation = 42° to 45°, axial displacement $\Delta l = 0.92 \text{ mm}$ to 0.98 mm, $\gamma = 1.26$ to 1.33, average elongation $\Delta l/l_0 = 0.15 - 0.16$, equivalent plastic strain at fracture based on average strain data $\epsilon_{eq}^p = 0.73-078$).

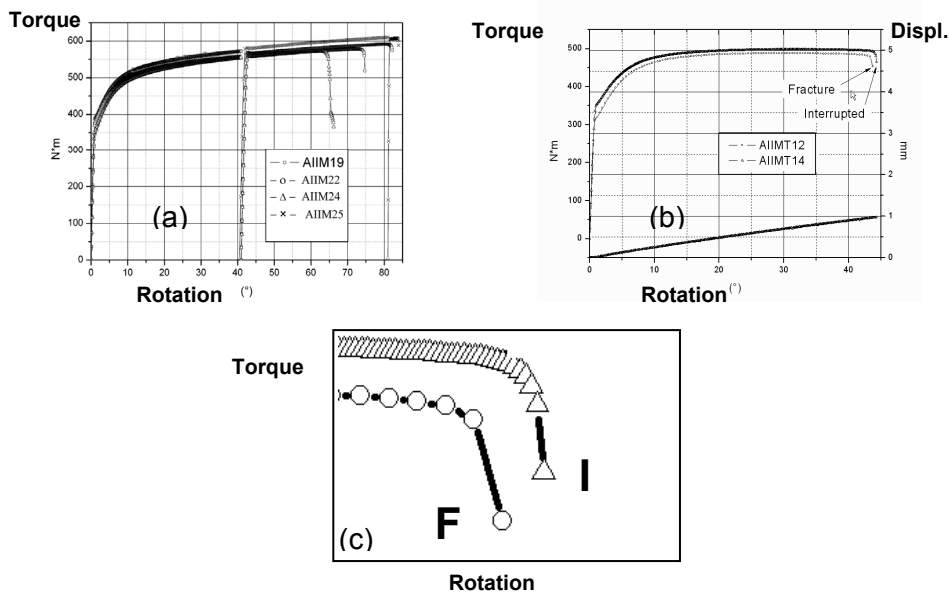


Figure 1 (a) Torque versus rotation curve for the T experiments. (b) Torque and axial displacement versus rotation curves for the TT experiments. (c) Softening part of the torque versus rotation curves for a fractured [F] and an interrupted [I] TT specimen.

Although it is well known that failure strains in T tests are very sensitive to surface stress concentrations, we have not yet identified the cause of the observed scatter in our experiments. The superimposed tensile stress in the TT experiments considerably reduces the equivalent strain at

failure (from 1.30 to 0.75). Figure 2c shows a small softening part of the loading curves for a fractured [F] and an interrupted [I] TT specimen. Such softening is also observed in the T experiments and may have two contributions: macroscopic geometric softening and microstructural damage softening, in particular by nucleation and growth of voids at inclusions and carbides. At large deformation levels in the T and TT experiments, we observe non uniform deformation along the specimen axis due to the end constraints of the grips on the relatively short specimen gage length. Towards the very end of the experiment, the small necking of the specimen (up to 2% of the initial diameter) and the localization of deformation in a narrow band (≈ 0.6 mm wide) occur in the non uniform deformation zone. Optical observations during the experiments show that formation of the narrow localization band coincides with the softening portion of the loading curve. We are investigating the processes governing softening of the band, in particular thermally activated relaxation of forest dislocations and cavity nucleation and growth at carbides. This latter point is discussed in the next section.

Fractographic observations

Figure 2 shows scanning electron microscope (SEM) photographs of the fracture surface of a T specimen and a TT-specimen. They demonstrate that fracture proceeds by nucleation, growth and coalescence of micro voids at carbides. The void distribution in the picture correlates well with the carbide distribution. The majority of the voids formed under pure shear (T specimen, Fig 2a) are elongated (with aspect ratio of 3-4 to 1) although patches of more equiaxed voids may also be found. In contrast, the fracture surface of the TT specimen contains more equiaxed voids while still showing evidence of shear deformation. Both T and TT fracture surfaces, display only an intriguingly low number of clearly identifiable carbides, raising the question of what happens to them during final fracture.

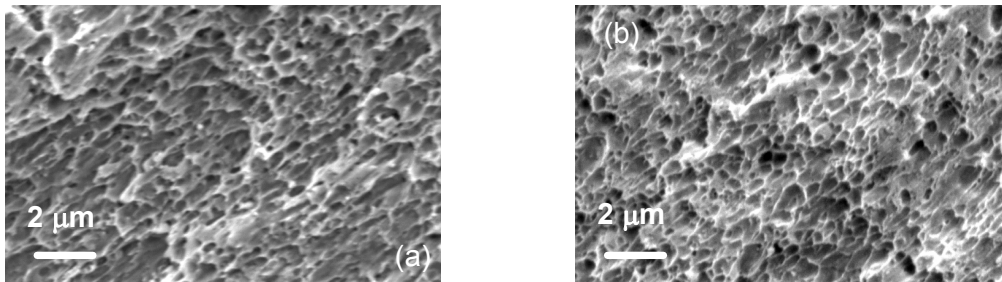


Figure 2 SEM photographs of the fracture surface of (a) a T specimen and (b) a TT specimen (shearing direction: top right to lower left).

At a somewhat larger scale than the void scale, the morphology of the fracture surface of the T specimen resembles that of a sheared deck of cards. Steps separating planes of localized shear appear to have been formed by tensile loading of the remaining ligament parallel to the shear planes. Other regions of the fracture surface appear smeared by the interference of fracture surface steps or asperities. Detailed SEM analyses of various sections of the fractured T and TT specimens demonstrate that failure initiates at the outside surface where strains are largest and propagates radially and circumferentially. Cross-sections of T and TT specimens unloaded before unstable fracture (that is, specimens unloaded after reaching point I of the softening part of the loading curve in Fig 1c) reveal no observable voids or micro cracks (except in one interrupted T test where we found a string of what appeared very shallow micro cracks). Cross sections perpendicular to the fracture surfaces of T, TT and tensile specimens revealed no collateral micro damage (i.e.

growing micro voids or micro cracks below the fracture plane) and only a few micro cracks and micro voids, a short distance ahead of arrested crack fronts, and collinear with the main crack plane.

4 DISCUSSION AND PRELIMINARY INTERPRETATION

The evidence presented in the preceding section suggests that ductile fracture under low triaxiality loading in the clean VAR steel tested in this research is dominated by void nucleation, growth and coalescence at carbides. Inspection of the fracture surfaces of tensile specimens shows that this is also the case for higher triaxialities. In the T and TT experiments, nucleation may be preceded or more likely associated with a strain localization and occurs in the very last stage of the total deformation. Incompatible strains between the heavily sheared matrix and rigid carbide afford the local stress elevation required to debond or break the carbides. Wedging of the voids by the strong and hard carbides they contain [4] or local tensile zones in the ligaments between two parallel but offset patches of sheared voids provide mechanisms for the growth of voids for predominantly shear loading with little or no stress triaxiality. Figure 3a illustrates the failure mechanism outlined here. A similar mechanism probably prevails in the TT specimens but with a stronger influence of the macroscopic tensile stress on the growth and coalescence of micro voids and hence on their more equiaxed appearance in the fracture surface (Fig 3b).

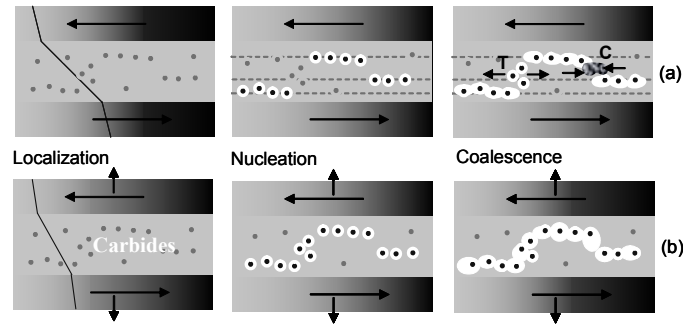


Figure 3 Schematic of failure process (a) in pure shear: note the tensile, T and compressive ligaments between shear planes; (b) under combined shear and tension (T = local tensile zone, C = local compressive zone because of interference).

The lack of observable nucleated and growing voids in cross sections of specimens loaded well into the softening region indicates that, once nucleated, neighboring voids grow and coalesce very quickly, with little additional global straining. The absence of collateral damage in broken tensile specimens suggests that this is also the case for loading at higher triaxialities. As a consequence, void nucleation is the key fracture process to model in order to predict fracture in these microstructures. That growth does not play an important role can be explained by observing that the mean distance between carbides is of the order of their size. Hence, defining the onset of coalescence as the point where nucleated micro voids at carbides start to interact, one sees that coalescence processes prevail as soon as voids are nucleated at neighboring carbides. The mechanism of void nucleation, whether by interface separation or by cracking of the carbides, is not yet established with certainty. Because of the submicron size of the carbides, at which voids nucleate, a model based on dislocation mechanics is required to calculate the local nucleation stress. In this work, we are investigating the model proposed by Kwon and Asaro [7] (on the basis of earlier work by Brown and Stobbs [8] and Goods and Brown [9]) to estimate the critical nucleation stress using our experimental deformation data. This model includes a contribution to

the local stress driven by plastic strain and one driven by the mean stress. Thus, it possesses two attractive features: that of being applicable to nucleation at submicron carbides, and that of treating states of stress of arbitrary triaxiality levels. From our experimental data, we calculate critical stresses for nucleation at carbides on the order of 1880 to 2140 MPa for TT and T experiments, respectively. These values are towards the higher end of values published in the literature, which is consistent with the fact that the mean carbide size is very small (0.23 μm). Thus the Kwon-Asaro model could provide a physically reasonable and practically manageable nucleation model to augment current void growth model in order to predict fracture in clean heat-treatable steels under more general loading conditions.

5 CONCLUSIONS AND FUTURE WORK

This investigation indicates that, in clean, strong and tough tempered steels, independent of the level of stress triaxiality, fracture is controlled by void nucleation at carbides, by cracking or decohesion of the particle. Void growth plays little role in the failure process, in the sense that it does not contribute in any significant way to the macroscopic toughness. A mechanism for the propagation of cracks by predominantly shear deformation has been outlined. The present results and their proposed interpretation are significant for fracture modeling and predictions in a broad class of steels. Our future work will focus on validating them further by performing 1) TT tests with higher tensile loads and notched round bar experiments, 2) numerical simulations of the experiments and 3) quantitative fractography of the localization and failure zone.

ACKNOWLEDGEMENTS

This work was performed with support from the Swiss National Science Foundation under Grant 2100-066777

REFERENCES

- [1] Gologanu M., Leblond J. B., Perrin G. and Devaux J. "Recent Extensions of Gurson's Model for Porous Ductile Metals", *"Continuum Micromechanics"*, P. Suquet, ed., CISM Lectures Series, Springer, New-York, 1997
- [2] Gologanu M. « Etude de quelques problèmes de rupture ductile des métaux » *Thèse de Doctorat de l'Université de Paris VI*, 1997
- [3] Pardoën T. and Hutchinson J. W. "An extended model for void growth and coalescence," *Journal of the Mechanics and Physics of Solids*, **48**, 2467-2512, 2000
- [4] Siruguet, K., "Rupture ductile à basse triaxialité effet des inclusions sur la croissance et la coalescence des cavités," *Thèse de doctorat*, Université Paris VI, 2000
- [5] Giovanola J. H. and Kirkpatrick, S. "Using the local approach to evaluate scaling effects in ductile fracture," *International Journal of Fracture*, **92**, 101-116, 1998
- [6] Giovanola, J. H., Kirkpatrick S. W. and Crocker J. E. "Fracture of Geometrically Scaled, Notched Three-Point-Bend Bars of High Strength Steel," *Eng. Fract. Mech.*, **62**, 291-310, 1999
- [7] Kwon, D. and Asaro, R.J. "A study of Void Nucleation, Growth, and Coalescence in Spheroidized 1518 Steel," *Metallurgical Transaction A*, **21A**, 117-134, 1990
- [8] Brown, L.M and Stobbs, W.M.. "The work-hardening of copper silicav. equilibrium plastic relaxation by secondary dislocations", *Philosophical Magazine*, **34**.351-372, 1976
- [9] Goods, S. H. and Brown, L. M. "The Nucleation of Cavities by Plastic Deformation," *Acta Met.*, **27**, 1-15, 1979